Quasiparticle density of states and triplet correlations in superconductor/ferromagnetic-insulator structures across a sharp domain wall

Alberto Hijano [1,2,*] Vitaly N. Golovach [1,3,4,†] and F. Sebastián Bergeret [1,3,‡]

[1] *Centro de Física de Materiales (CFM-MPC) Centro Mixto CSIC-UPV/EHU, E-20018 Donostia-San Sebastián, Spain*

[2] *Department of Condensed Matter Physics, University of the Basque Country UPV/EHU, 48080 Bilbao, Spain*

[3] *Donostia International Physics Center (DIPC), 20018 Donostia–San Sebastián, Spain*

[4] *IKERBASQUE, Basque Foundation for Science, 48011 Bilbao, Spain*

(Received 24 February 2022; revised 19 April 2022; accepted 25 April 2022; published 6 May 2022)

A ferromagnetic insulator (FI) in contact with a superconductor (S) is known to induce a spin splitting of the BCS density of states at the FI/S interface. This spin splitting causes the Cooper pairs to reduce their singlet-state correlations and acquire odd-in-frequency triplet correlations. We consider a diffusive FI/S bilayer with a sharp magnetic domain wall in the FI, and we study the local quasiparticle density of states and triplet superconducting correlations. In the case of collinear alignment of the domains, we obtain analytical results by solving the Usadel equation. For a small enough exchange field or weak superconductivity, we also find an analytical expressions for arbitrary magnetic textures, which reveals how the triplet component vector depends on the local magnetization of the FI. For an arbitrary angle between the magnetizations and the strength of the exchange field, we numerically solve the problem of a sharp domain wall. We finally propose two different setups based on FI/S/F stacks, where F is a ferromagnetic layer, to filter out singlet pairs and detect the presence of triplet correlations via tunneling differential conductance measurements.

DOI: 10.1103/PhysRevB.105.174507

I. INTRODUCTION

The exchange coupling at the interface between a ferromagnetic insulator (FI) and a thin superconducting layer (S) can lead to a spin-splitting of the density of states (DOS) in the S layer, as observed in numerous experiments [1–5]. Recently, there has been a renewed interest in these systems due to various proposed applications. These applications include spin valves [6,7], spin batteries [8,9], magnetometers [10,11], thermometers [12,13], caloritronic devices [14–16], thermoelectric elements [17,18], and radiation detectors [19,20]. FI/S structures have also been explored in the context of Majorana fermions in semiconducting wires [21–23].

Most of these applications require a robust superconducting gap with a sizable spin-splitting. This can be achieved, for example, in EuS/Al systems [2,4,5,7,24], where the interfacial exchange interaction leads to a sharp spin-splitting in S layers with thicknesses smaller than the coherent length. On the theoretical side, the effect of the interfacial exchange field and the induced spin-splitting on the superconducting state has been studied in numerous works [5,25–27]. Most of these works assume a homogeneous spin-splitting field. This assumption is justified, even in a multidomain situation, if the characteristic domain size of EuS is much longer than the superconducting coherence length ξ_0.

There are, however, situations in which the domain size may be of the order of the superconducting coherence length. The effect of domain walls in magnetic and insulating ferromagnets on adjacent superconductors has been studied theoretically [28–32] and experimentally [4,33], while Ref. [34] studied the influence of domain-wall dynamics on superconductivity. In particular, Ref. [4] provided experimental evidence that EuS consists of multiple domains with a size of the order of the coherence length of the Al layer attached to it. The authors of that work contrast spectroscopic measurements with a theoretical model that assumed alternating up/down domains of different sizes. In the present work, we generalize this approach and study a FI/S structure with two noncollinear magnetic domains.

Despite the amount of experimental work on FI/S systems, almost all of it focuses on studying its quasiparticle spectrum. There is, however, an interesting aspect that is not often mentioned in these works. The mere existence of an interfacial exchange field leads to conversion of singlet superconducting correlations to triplet ones [35–38]. The induced triplet component has a total zero spin projection if the FI consists of a single domain with homogeneous magnetization. However, in FI/S systems with noncollinear magnetization, triplet components with different spin-projections may coexist with the singlet one.

In this work, we study the equilibrium properties of a FI/S bilayer with a sharp domain wall separating two magnetic domains. We present an analytical solution for the Usadel equation for a FI/S bilayer consisting of two semi-infinite magnetic domains with collinear magnetization and noncollinear magnetization in the weak exchange field limit,

*alberto.hijano@ehu.eus

†vitaly.golovach@ehu.eus

‡fs.bergeret@csic.es

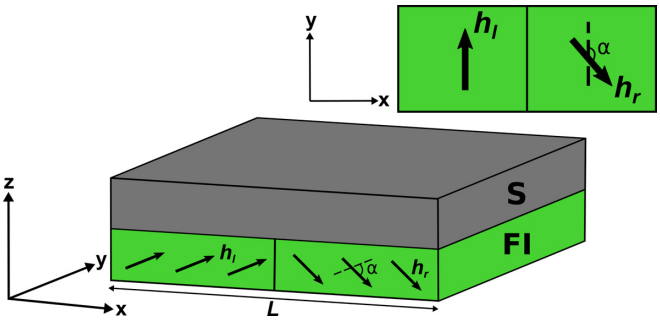

FIG. 1. Schematic view of the S/FI structure under consideration. The ferromagnetic insulator has two domains with arbitrary in-plane magnetization direction. The inset shows the top view of the FI. The magnetizations of the two domains lie on the xy plane, and they form an angle α.

and we use numerical methods to solve the noncollinear case with arbitrary exchange field strength. Additionally, we study the spatial evolution of the triplet correlations near a domain wall, and we propose a method to detect them using tunneling spectroscopy of an additional ferromagnetic layer. The work is organized as follows: In Sec. II we present the main equations describing a diffusive superconductor attached to a FI layer with multiple domains and a general Lagrangian from which one can derive the Usadel equation. We identify conserved quantities within each domain. In Sec. III we use these integrals of motion to derive an analytical expression for the DOS of a FI/S system with two collinear domains of arbitrary magnitude. In Sec. IV we generalized these results to the case of noncollinear magnetization. Finally, in Sec. V we study the properties and spatial evolution of the triplet correlations, and we suggest a way to detect them. We summarize the results in Sec. VI.

II. THE MODEL

We consider a FI/S bilayer structure; see Fig. 1. A diffusive superconducting film is placed on top of a FI film. A typical example is Eu/Al studied in several papers [2,4,5,7,24]. In these systems the EuS film is polycrystalline, and magnetic domains with sharp boundaries are very common, particularly before the first magnetization of the EuS [4].

To describe the system, we use the quasiclassical Green's function (GF) formalism extended to treat spin-dependent fields [35]. In this case, the GF $\check{g}$ is a 4×4 matrix in Nambu-spin space. In the diffusive limit, it does not depend on momentum and is determined by the Usadel equation [39]. The interfacial exchange field is introduced as an effective boundary condition at the FI/S interface [38,40,41]. Assuming that the thickness of the S layer is smaller than the coherence length, one can integrate the Usadel equation over the thickness to reduce the dimension of the problem. The resulting Usadel equation for the retarded GF reads

$$D\nabla \cdot (\check{g}\nabla\check{g}) + [i\varepsilon\tau_3 - i\boldsymbol{h}\cdot\boldsymbol{\sigma}\tau_3 - \check{\Delta}, \check{g}] = 0, \tag{1}$$

where $\nabla = (\partial_x, \partial_y)$, D is the diffusion constant, ε is the energy, $\boldsymbol{h}$ is the effective exchange field stemming from the interface, and $\check{\Delta} = \Delta\tau_1$ is the order parameter. The exchange field is only finite at the FI/S interface, and we approximate it as $|\boldsymbol{h}_{\rm int}| = h_{\rm int}a\delta(z)$, where $h_{\rm int}(x, y)$ is the exchange field at the interface, and a is the thickness of an effective layer over which the exchange interaction is finite [38,42]. After integration over the z direction, the effective exchange field is given by $h = h_{\rm int}a/d$ [5]. It is worth noting that the critical temperature of the S layer decreases with decreasing thickness, such that at low temperatures superconductivity can be fully suppressed when $h > \Delta/\sqrt{2}$ [43,44]. In this work, we consider values of the exchange field that are weak enough such that superconducting ordering and the exchange field coexist. The matrices σ_i (τ_i), $i = 1, 2, 3$, in Eq. (1) are the Pauli matrices in the spin (Nambu) space. The general structure of $\check{g}$ is

$$\check{g} = \hat{g}\tau_3 + \hat{f}\tau_1, \tag{2}$$

where $\hat{g}$ and $\hat{f}$ are the normal and anomalous GF in spin-space.

The GF satisfies the normalization condition $\check{g}^2 = 1$, and it can be parametrized with the help of the generalized θ-parametrization [45],

$$\check{g} = (\cos\theta V_0 - \sin\theta\boldsymbol{V}\cdot\boldsymbol{\sigma})\tau_3 + (\sin\theta V_0 + \cos\theta\boldsymbol{V}\cdot\boldsymbol{\sigma})\tau_1, \tag{3}$$

which is described by two scalars θ and V_0 and the vector $\boldsymbol{V}$. V_0 and $\boldsymbol{V}$ satisfy the condition

$$V_0^2 + \boldsymbol{V}^2 = 1. \tag{4}$$

V_0 and $\boldsymbol{V}$ describe the singlet and triplet correlations, respectively. If $\boldsymbol{h}$ is homogeneous, then $\boldsymbol{V}$ is parallel to it, but in general, as we show on Sec. V, $\boldsymbol{V}$ is not parallel to the local exchange field.

In the above parametrization, the Usadel equation reduces to the following set of equations:

$$D\nabla^2\theta + 2i\varepsilon\sin\theta V_0 - 2i\cos\theta\boldsymbol{h}\cdot\boldsymbol{V} + 2\Delta\cos\theta V_0 = 0, \tag{5a}$$

$$D(V_0\nabla^2\boldsymbol{V} - \boldsymbol{V}\nabla^2 V_0) + 2i\varepsilon\cos\theta\boldsymbol{V} - 2i\sin\theta\boldsymbol{h}V_0 - 2\Delta\sin\theta\boldsymbol{V} = 0. \tag{5b}$$

It is useful for finding analytical solutions to write a Lagrangian that leads to Eqs. (5) as the Euler-Lagrange equations:

$$\mathcal{L} = \frac{D}{2}\sum_\mu(\nabla V_\mu)^2 + \frac{D}{2}(\nabla\theta)^2 + 2i\varepsilon\cos\theta V_0 + 2i\sin\theta\boldsymbol{h}\cdot\boldsymbol{V} - 2\Delta\sin\theta V_0, \tag{6}$$

with $\mu = 0, 1, 2, 3$. This Lagrangian coincides with the form of the nonlinear σ-model from which the Usadel equation can also be derived [46,47].

The above equations are valid for arbitrary magnetic textures. In the following, we focus on the situation of two semi-infinite magnetic domains with constant magnetization. The domains are separated by a sharp domain wall at $x = 0$ with a length much smaller than the superconducting coherence length. We assume that one of the domains ($x < 0$) is polarized along the y axis, whereas the magnetization of the

other domain ($x > 0$) forms an angle α with the y axis; see Fig. 1. At distances much larger than the coherence length, the GF takes its bulk form. The system has translational symmetry along the y and z directions, so the parameters only depend on the x coordinate.

On each domain, the Lagrangian (6) does not depend explicitly on the position $\boldsymbol{r}$, so the corresponding Hamiltonian is an integral of motion in each domain. The conserved quantity is namely given by

$$\mathcal{E} = \frac{D}{2}\sum_{\mu}(\nabla V_\mu)^2 + \frac{D}{2}(\nabla\theta)^2 - 2i\varepsilon\cos\theta V_0 - 2i\sin\theta \boldsymbol{h}\cdot\boldsymbol{V} + 2\Delta\sin\theta V_0. \tag{7}$$

The values of $\mathcal{E}$ far away from the domain wall, where the GF is given by the bulk solution and therefore is constant in space, can be easily obtained:

$$\mathcal{E} = -2i\varepsilon\cos\bar{\theta}\bar{V}_0 - 2i\sin\bar{\theta}\boldsymbol{h}\cdot\bar{\boldsymbol{V}} + 2\Delta\sin\bar{\theta}\bar{V}_0, \tag{8}$$

where the bulk values $\bar{\theta}$ and $\bar{\boldsymbol{V}}$ of the GF are given by the inverse relations of Eq. (2),

$$\tan\theta = \frac{f_0}{g_0}, \tag{9a}$$

$$\boldsymbol{V} = -\frac{\boldsymbol{g}}{\sin\theta}, \tag{9b}$$

$$V_0 = \frac{g_0}{\cos\theta}, \tag{9c}$$

and the bulk GF is given by

$$\hat{\check{g}} = \frac{-i(\varepsilon - \boldsymbol{h}\cdot\boldsymbol{\sigma})}{\sqrt{\Delta^2 - (\varepsilon - \boldsymbol{h}\cdot\boldsymbol{\sigma})^2}}, \tag{10a}$$

$$\hat{\check{f}} = \frac{\Delta}{\sqrt{\Delta^2 - (\varepsilon - \boldsymbol{h}\cdot\boldsymbol{\sigma})^2}}, \tag{10b}$$

with $\hat{g} = g_0 + \boldsymbol{g}\cdot\boldsymbol{\sigma}$, $\hat{f} = f_0 + \boldsymbol{f}\cdot\boldsymbol{\sigma}$. In the following section, we use these expressions to define integrals of motion that allow for an analytical solution when the magnetic domains are collinear.

III. DOMAINS WITH COLLINEAR MAGNETIZATION

If the magnetization of the two domains is collinear, the problem can be greatly simplified. First, only the component of the vector $\boldsymbol{V}$ parallel to the magnetization is nonzero. Without any loss of generality, we assume that the magnetizations lie in the z axis, such that $V_1 = V_2 = 0$. In this case, Eq. (5) reads

$$D\theta'' + 2i\varepsilon\sin\theta\cos\theta_3 - 2ih\cos\theta\sin\theta_3 + 2\Delta\cos\theta\cos\theta_3 = 0, \tag{11a}$$

$$D\theta_3'' + 2i\varepsilon\cos\theta\sin\theta_3 - 2ih\sin\theta\cos\theta_3 - 2\Delta\sin\theta\sin\theta_3 = 0, \tag{11b}$$

where $V_3 = \sin\theta_3$. One can combine these equations to obtain two decoupled equations for each spin component:

$$D\theta_\pm'' + 2i\varepsilon\sin\theta_\pm \mp 2ih\sin\theta_\pm + 2\Delta\cos\theta_\pm = 0, \tag{12}$$

where $\theta_\pm = \theta \pm \theta_3$, respectively, describe the spin-up and -down components of the GF.

Since the problem is decoupled in spin space, one can derive equations in (12) from two independent Lagrangians:

$$\mathcal{L}_\pm = \frac{D}{2}{\theta_\pm'}^2 + 2i\varepsilon\cos\theta_\pm \mp 2ih\cos\theta_\pm - 2\Delta\sin\theta_\pm. \tag{13}$$

Because $\mathcal{L}_\pm$ do not depend explicitly on x, the following quantities are conserved in space:

$$\mathcal{E}_\pm = \frac{D}{2}{\theta_\pm'}^2 - 2i\varepsilon\cos\theta_\pm \pm 2ih\cos\theta_\pm + 2\Delta\sin\theta_\pm. \tag{14}$$

These expressions can be evaluated at the bulk where the spatial derivative vanishes and the GF is given by the bulk solution [see Eq. (10)]. $\cos\theta_\pm$ and $\sin\theta_\pm$ are given by the spin components $\hat{g}$ and $\hat{f}$, respectively, where the $\pm$ sign corresponds to the up/down spin index,

$$\mathcal{E}_\pm = 2\sqrt{\Delta^2 - (\varepsilon \mp h)^2} = \frac{2\Delta}{\sin\bar{\theta}_\pm}. \tag{15}$$

Here $\bar{\theta}_\pm$ are the values of $\theta_\pm$ at the bulk. In the following, we omit the spin subscript to simplify the notation. Substituting Eq. (14) into (15) and applying trigonometric identities, we arrive at

$$\sin\bar{\theta}\frac{D}{8\Delta}{\theta'}^2 = \sin^2\frac{\theta - \bar{\theta}}{2}. \tag{16}$$

Equation (16) does not explicitly contain the independent variable x. Taking the square root on both sides of the equation, we obtain a first-order differential equation that can be integrated to obtain

$$\tan\frac{\theta - \bar{\theta}_{l/r}}{4} = \begin{cases} c_l e^{x/\lambda_l}, & x \leqslant 0, \\ c_r e^{-x/\lambda_r}, & x \geqslant 0, \end{cases} \tag{17}$$

where $\lambda_{\pm,l/r}^2 = D/[2\sqrt{\Delta^2 - (\varepsilon \mp h_{l/r})^2}]$ is chosen such that $\mathrm{Re}\{\lambda_{l/r}\} > 0$, and that the exponential functions decay away from the domain wall. $h_{l/r}$ is the value of the exchange field in the left ($x < 0$) and right ($x > 0$) domains.

From Eq. (17) one can obtain the spatial dependence of $\theta(x)$ by determining the constants $c_{l,r}$. For this we use the fact that the GF and its derivative are continuous at the domain wall. Applying this condition, we obtain the values of the constants in Eq. (17),

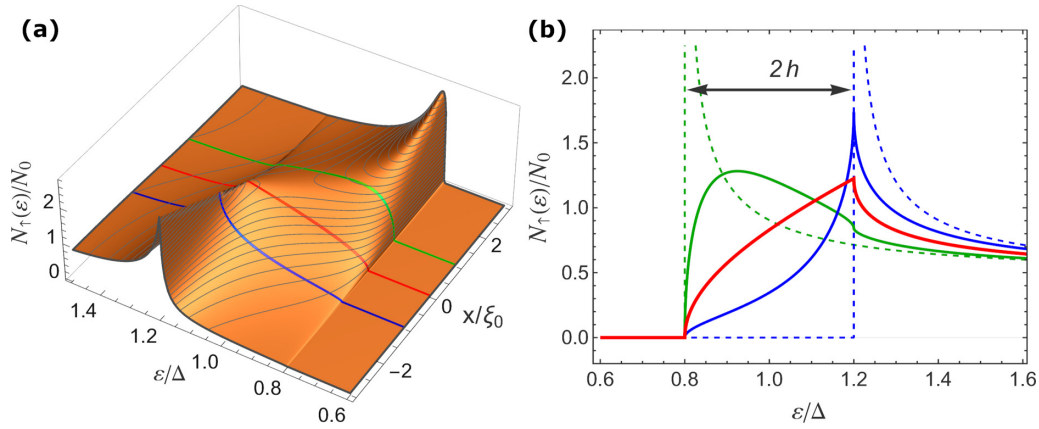

FIG. 2. Local DOS (for spin-up) of the superconductor film for domains with opposite magnetization strength and effective exchange field $h = 0.2\Delta$. The line traces of the right panel are taken at $x = -\xi_0$ (blue), $x = 0$ (red), and $x = \xi_0$ (green). The dashed lines show the BCS spin-splitting of the DOS deep inside of the domains $x \to -\infty$ (blue) and $x \to \infty$ (green).

$$c_{l/r} = \mp \frac{\frac{\lambda_{l/r}}{\lambda_{r/l}}\left(1-\tan^2\frac{\Delta\theta}{4}\right)+1+\tan^2\frac{\Delta\theta}{4} - \sqrt{\left[\frac{\lambda_{l/r}}{\lambda_{r/l}}\left(1-\tan^2\frac{\Delta\theta}{4}\right)+1+\tan^2\frac{\Delta\theta}{4}\right]^2 + \frac{4\lambda_{l/r}^2}{\lambda_{r/l}^2}\tan^2\frac{\Delta\theta}{4}}}{2\frac{\lambda_{l/r}}{\lambda_{r/l}}\tan\frac{\Delta\theta}{4}}, \tag{18}$$

where $\Delta\theta = \theta_r - \theta_l$, and the upper and lower signs correspond to the left and right domains, respectively. The sign of the square root on Eq. (18) is chosen such that the DOS is positive and the solution is physically meaningful. Setting the order parameter to zero in the right domain and the exchange fields to zero, we recover the results by Altland *et al.* [48] for a singlet S/N junction. Golubov *et al.* [49] also followed a similar procedure to study the DOS at ferromagnetic and normal layers on S(FN) and S(FF) structures.

Equation (17) together with Eq. (18) determine the analytical solution for the two semi-infinite collinear domains. The local DOS is related to the GF through the expression

$$\frac{N(\varepsilon)}{N_0} = \frac{1}{2}\mathrm{Re}\{\mathrm{Tr}\,\hat{g}(\varepsilon)\} = \frac{1}{2}\mathrm{Re}\{\cos\theta_+ + \cos\theta_-\}. \tag{19}$$

As a first example, we assume that the magnetizations of the two domains are opposite in direction but equal in amplitude ($h_l = -h_r = h$). In this case, the DOS at the domain wall ($x = 0$) has a simple form

$$\frac{N(\varepsilon)}{N_0} = \mathrm{Re}\left\{\frac{\sqrt{\Delta^2-(\varepsilon-h)^2}-\sqrt{\Delta^2-(\varepsilon+h)^2}}{2ih}\right\}, \tag{20}$$

which leads to the red curves in Fig. 2. This analytical result coincides with the numerical result obtained in Refs. [4,32] for a narrow domain wall between two collinear domains. In Fig. 2, we show the spatial dependence of the DOS for spin-up electrons in the antiparallel magnetization configuration. Far from the domain wall, the coherent peaks of the DOS are well-defined (dashed lines). The presence of the domain wall smears the peak. In Fig. 3(a) we show the spatial dependence of the full DOS. Specifically, Fig. 3(b) shows the DOS at the values of x indicated by the colored lines in panel (a). The magnitude of the exchange field is the same on both domains so the total DOS is symmetric with respect to $x = 0$. For large enough distances away from the domain wall, the BCS peak is shifted by the exchange field to $\varepsilon = \Delta \pm h$. Near the domain wall, there is a crossover between the position of the spin-up/spin-down peaks over a length scale of the order of the superconducting coherence length $\xi_0 = \sqrt{D/\Delta}$. Notice that around the domain wall, the inner peak is broader and lower than the outer peak [see Fig. 3(b)], but the gap edge remains, as expected, at $\varepsilon < \Delta - h$.

A second interesting example is when the exchange field is only finite in one of the regions ($x < 0$). This corresponds to an S layer only partly covered by the the FI layer. In Fig. 3(c), we show the local DOS in this case. The spin-split DOS at $x \ll -\xi_0$ evolves into the usual BCS DOS at $x \gg \xi_0$, over the length ξ_0 around the domain wall. The splitting of the DOS peaks does not decrease smoothly, as one would expect in a system in which the exchange field is suppressed gradually over a length much larger than ξ_0. Namely, the inner peak is smeared in a similar way to the antiparallel magnetization case [Fig. 3(b)], such that the DOS has the same "shark-fin" shape right at $x = 0$ [red curve in Fig. 3(d)]. All of the above predictions could be proven by performing local tunneling spectroscopy measurements.

IV. NONCOLLINEAR MAGNETIZATION

In the previous section, we focused on the collinear magnetization case in which it was possible to decouple the components of the Usadel equation. In that case, we can find conserved quantities, Eq. (15), and we obtain analytically expressions for the GF. If the magnetizations are noncollinear, the system lacks enough symmetries to reduce the number of coupled equations. Nonetheless, it is possible to solve the Usadel equation (5) analytically in the weak superconducting

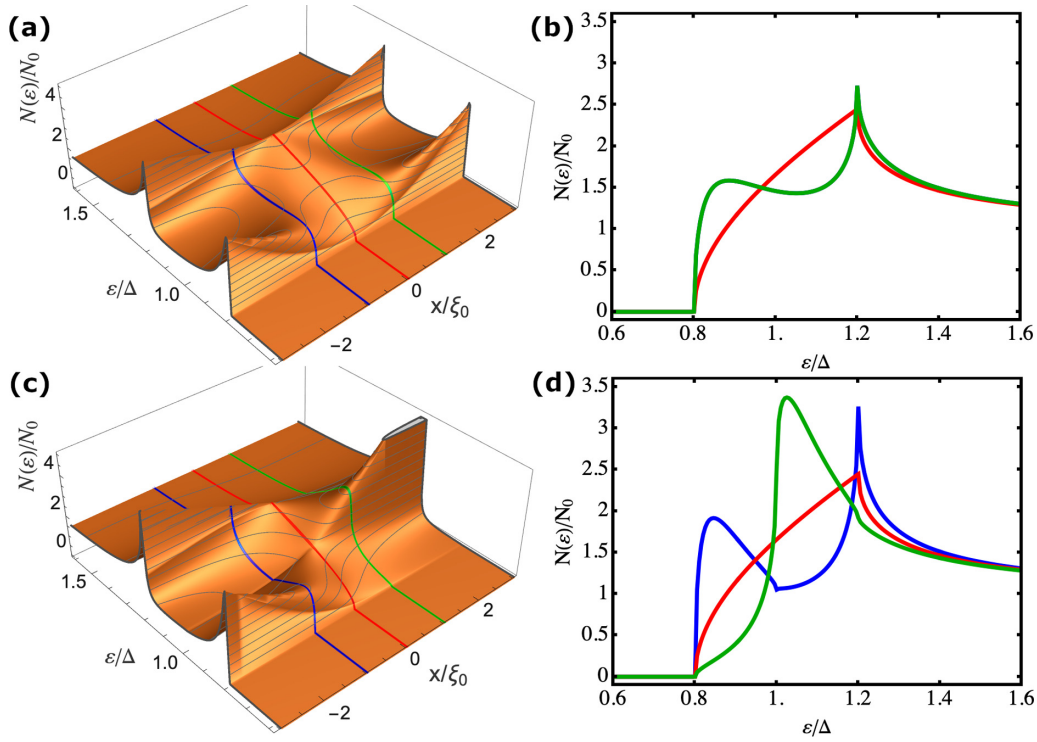

FIG. 3. Local DOS of the S layer for (a,b) $h_l = 0.2\Delta$ and $h_r = -0.2\Delta$, and (c,d) $h_l = 0.2\Delta$ and $h_r = 0$. The color lines in the right panels are taken at $x = -\xi_0$ (blue), $x = 0$ (red), and $x = \xi_0$ (green).

or weak exchange field limits, as discussed in the next subsections. Later below, we study the two-domain situation for an arbitrarily large exchange field numerically [50].

A. Weak superconductivity

If the superconductor is close to the critical temperature T_c, the Usadel equation (5) can be linearized for a small order parameter ($\Delta \ll T, h$). This limit is very illustrative to understand the lengthscales involved in the system.

Near T_c the GF can be approximated by $\check{g} = \tau_3 + \hat{f}\tau_1$. The linearized Usadel equation determines the anomalous GF $\hat{f}$,

$$\frac{D}{2} f_0'' + i\varepsilon f_0 - i\boldsymbol{h}\cdot\boldsymbol{f} + \Delta = 0, \tag{21a}$$

$$\frac{D}{2}\boldsymbol{f}'' + i\varepsilon\boldsymbol{f} - i\boldsymbol{h} f_0 = 0, \tag{21b}$$

where the spin structure is

$$\hat{f} = f_0 + \sum_{j=1,3} f_j \sigma_j, \tag{22}$$

where f_0 is the singlet, and f_j, $j = 1, 2, 3$, are the triplet components. For the two semi-infinite domain structures considered in this work, the solution to Eq. (21) is given by

$$f_0 = \overline{f}_0 + c_+ e^{-q_+|x|} + c_- e^{-q_-|x|}, \tag{23a}$$

$$\boldsymbol{f} = \overline{\boldsymbol{f}} + i\boldsymbol{h}\sum_{j=\pm} \frac{c_j}{q_j^2 D/2 + i\varepsilon} e^{-q_j|x|} + \boldsymbol{d}\, e^{-q|x|}, \tag{23b}$$

where $\overline{f}_0$ and $\overline{\boldsymbol{f}}$ are the asymptotic values at $x = \pm\infty$ of the singlet and triplet components, respectively, and $q_\pm^2 = -2i(\varepsilon \mp h)/D$, $q^2 = -2i\varepsilon/D$. The triplet can be written as the sum of the component parallel to the local exchange field [second term in Eq. (23b)], and the component orthogonal to it proportional to the vector $\boldsymbol{d}$, with $\boldsymbol{h}\cdot\boldsymbol{d} = \boldsymbol{0}$. The component perpendicular to the local exchange field decays away from the domain wall over the length $\xi_\varepsilon = \mathrm{Re}\{q\}^{-1}$, whereas the correction to the bulk (parallel) solution is significant at distances less than $\xi_h = \mathrm{Re}\{q_+\}^{-1} = \mathrm{Re}\{q_-\}^{-1}$.

B. Weak exchange field

Another analytical limiting case is the case of a weak exchange field ($|\boldsymbol{h}| \ll \Delta$). In this case, one can linearize the Usadel equation (5) and solve the system for an arbitrary magnetization texture. In zeroth order in $\boldsymbol{h}$, only the singlet component of the GF is finite and it is given by Eqs. (9) and (10) setting $\boldsymbol{h} = \boldsymbol{0}$,

$$\tan\theta = \frac{\Delta}{-i\varepsilon}, \tag{24a}$$

$$V_0 = 1. \tag{24b}$$

To first order in $\boldsymbol{h}$, both θ and V_0 are not corrected, whereas the triplet vector $\boldsymbol{V}$ is determined by

$$\boldsymbol{V}'' - \lambda^{-2}\boldsymbol{V} = \frac{2i\Delta}{D\sqrt{\Delta^2 - \varepsilon^2}}\boldsymbol{h}(x'), \tag{25}$$

where $\lambda^2 = D/(2\sqrt{\Delta^2 - \varepsilon^2})$ ($\mathrm{Re}\{\lambda\} > 0$) is the energy-dependent coherence length. The solution of this equation can be written as

$$\boldsymbol{V} = \int dx' G(x, x') \frac{2i\Delta}{D\sqrt{\Delta^2 - \varepsilon^2}}\boldsymbol{h}, \tag{26}$$

where $G(x, x')$ is the Green's function of the differential equation (25) determined by

$$\left(\partial_x^2 - \lambda^{-2}\right)G(x, x') = \delta(x - x'). \tag{27}$$

Solving Eq. (27), we arrive at

$$\boldsymbol{V}(x) = \frac{-i\Delta}{\sqrt{2D}(\Delta^2 - \varepsilon^2)^{3/4}} \int dx' e^{-|x-x'|/\lambda} \boldsymbol{h}(x'). \tag{28}$$

This result shows explicitly the spatial dependence of the triplet vector. It is determined by the exchange field averaged over the length λ. For example, if the spatial variation of the exchange field $\boldsymbol{h}(x)$ is slower than the length λ, then the vector $\boldsymbol{V}$ is locally parallel to the exchange field. In particular, in the case of two magnetic domains separated by a smooth (with respect to the length λ) domain wall, the vector $\boldsymbol{V}$ is always aligned with the local field $\boldsymbol{h}$.

In this work, we are mainly interested in sharp domain walls, i.e., domain walls with sizes much smaller than λ. If we model such a situation by a steplike exchange field with $\boldsymbol{h} = \boldsymbol{h}_l\theta(-x) + \boldsymbol{h}_r\theta(x)$, then the triplet vector at the left and right sides of the domain wall can be obtained from Eq. (28):

$$\boldsymbol{V}_{l/r} = \frac{-i\Delta}{2(\Delta^2 - \varepsilon^2)}[2\boldsymbol{h}_{l/r} + (\boldsymbol{h}_{r/l} - \boldsymbol{h}_{l/r})e^{-|x|/\lambda}]. \tag{29}$$

As expected, at distances much larger than λ from the domain wall, $\boldsymbol{V}$ is parallel to the local exchange field. In contrast, the transverse component to the field is maximized at the domain wall and decays over λ away from it. The above analytical results are obtained for weak exchange fields. In the next section, we consider an arbitrarily strong exchange field.

C. Arbitrary exchange field

In this section, we consider two domains with an arbitrarily large exchange field and an arbitrary angle between the domain magnetizations, and we solve numerically the Usadel equation. For this it is convenient to differentiate twice Eq. (4) and substitute the result into Eq. (5). We thus arrive at [32,51]

$$D\theta'' + 2i\varepsilon \sin\theta V_0 - 2i\cos\theta \boldsymbol{h}\cdot\boldsymbol{V} + 2\Delta\cos\theta V_0 = 0, \tag{30a}$$

$$D\boldsymbol{V}'' + D\boldsymbol{V}\left(V_0'^2 + \boldsymbol{V}'^2\right) + 2i\sin\theta((\boldsymbol{h}\cdot\boldsymbol{V})\boldsymbol{V} - \boldsymbol{h}) - 2(-i\varepsilon\cos\theta + \Delta\sin\theta)V_0\boldsymbol{V} = 0, \tag{30b}$$

$$DV_0'' + DV_0\left(V_0'^2 + \boldsymbol{V}'^2\right) + 2i\sin\theta\boldsymbol{h}\cdot\boldsymbol{V}V_0 + 2(-i\varepsilon\cos\theta + \Delta\sin\theta)\left(1 - V_0^2\right) = 0. \tag{30c}$$

We solve the above equations numerically for an S layer of finite length L. The domain wall is located at $x = 0$. The spectral current vanishes at the boundaries with vacuum. In the generalized θ-parametrization, this translates into the following boundary conditions for Eq. (30):

$$\theta'|_{x=\pm L/2} = 0, \tag{31a}$$

$$\boldsymbol{V}'|_{x=\pm L/2} = 0, \tag{31b}$$

$$V_0'|_{x=\pm L/2} = 0. \tag{31c}$$

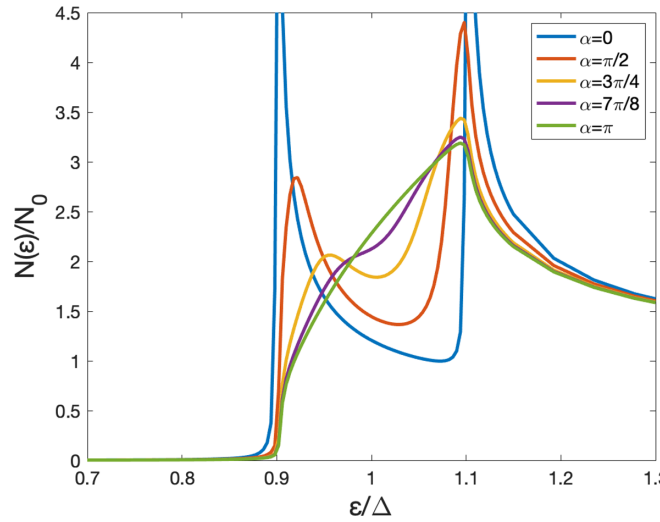

FIG. 4. Density of states at the domain wall for different values of the angle α between the domains' magnetizations.

In Fig. 4 we show the computed total DOS at the domain wall for domains with the same exchange field magnitude $h = 0.1\Delta$ and different orientations (see Fig. 1). In the $\alpha = 0$ case, the exchange field is uniform along the sample, so the DOS is the homogeneous spin-split BCS. Both peaks are broadened and lowered by increasing α, and the DOS exhibits the "shark-fin" when the magnetizations are antiparallel. The spin-splitting is still visible up to values of $\alpha \approx 7\pi/8$.

V. TRIPLET PAIR CORRELATIONS IN FI/S STRUCTURES AND THEIR DETECTION

In the previous sections, we analyzed the quasiparticle spectrum. Here we focus on another aspect of the FI/S structures: the superconducting triplet pair-correlations. These appear due to the finite interfacial exchange field that converts a conventional singlet into triplet pairs [35,52].

Within our model, pair correlations are described by the anomalous component $\hat{f}$ introduced in Eq. (2), which in the spin-space has the general structure given by Eq. (22). Because we consider the strict diffusive limit, all components of $\hat{f}$ are isotropic in momentum (s-wave symmetry). From the Fermi statistics for fermion pairs, it follows that f_0 is an even function of frequency whereas f_j are odd [35,53–55]. The following association between the different components of the condensate and the spin state of electron pairs can be made [56]:

$$(\uparrow\downarrow - \downarrow\uparrow) \leftrightarrow 2f_0, \tag{32}$$

$$-(\uparrow\uparrow - \downarrow\downarrow) \leftrightarrow 2f_1, \tag{33}$$

$$(\uparrow\uparrow + \downarrow\downarrow) \leftrightarrow 2if_2, \tag{34}$$

$$(\uparrow\downarrow + \downarrow\uparrow) \leftrightarrow 2f_3. \tag{35}$$

In other words, each triplet component of the condensate is associated with maximally entangled states. In a conventional BCS superconductor, only the singlet component f_0 is finite. Triplet components are finite in the presence of an exchange

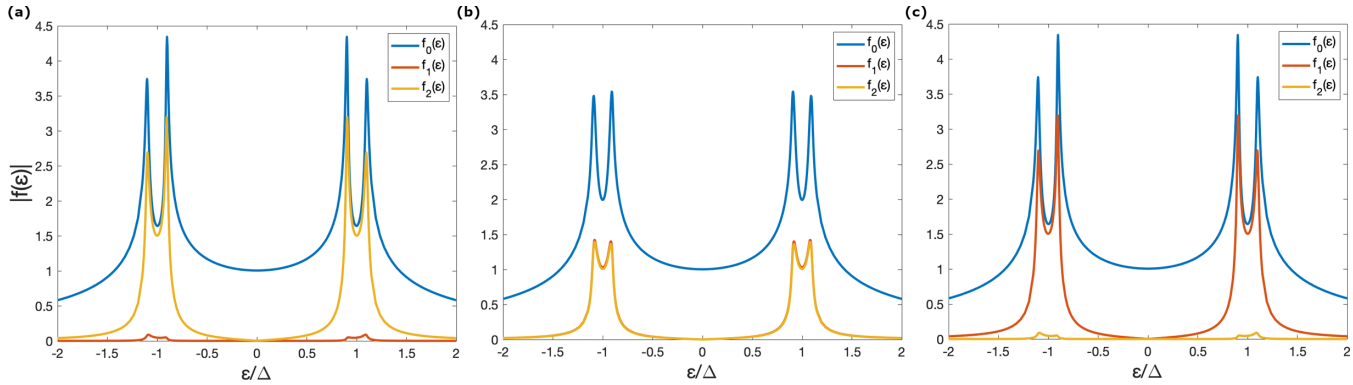

FIG. 5. The spectral weight of the singlet and triplet components of $\hat{f}$ at different points in the superconductor: (a) $x = -5\xi_0$, (b) $x = 0$, and (c) $x = 5\xi_0$. We have chosen $\alpha = \pi/2$, $L = 10\xi_0$, and $h_{l/r} = 0.1\Delta$.

field. In a homogeneous case, we choose the spin quantization axis along the magnetization direction, e.g., the z axis. The only finite components of the condensates are, in this case, f_0 and f_3. All triplet components may appear in a multidomain situation with arbitrary magnetization directions.

Here we study the singlet and triplet correlations in a FI/S bilayer with two noncollinear domains; see Fig. 1. We assume that $\alpha = \pi/2$ such that two components f_1, f_2 are finite. The length of S is $L = 10\xi_0$. In Fig. 5 we show the spatial dependence of the singlet and triplet components of $\hat{f}$ for all energies, calculated numerically. All condensate components show peaks at $|\varepsilon| = \Delta \pm h$ and decay to zero at energies much larger than the gap. Inside the gap, the amplitude of the singlet is of the order of 1. In contrast, at $\varepsilon = 0$ the triplet components are of the order of Γ/Δ, where Γ is the Dynes parameter [57] describing inelastic scattering. They increase linearly at small energies and become comparable to the singlet component within the range $|\varepsilon| \in [\Delta - h, \Delta + h]$. Far away from the domain wall, only the triplet component parallel to the local exchange field is finite. Both components, f_1 and f_2, have the same magnitude at the domain wall, as anticipated from our analytical result, Eq. (28). In Fig. 6(a), we show the spatial dependence of the triplet correlations at $\varepsilon = \Delta - h$. The length over which the triplet components change is of the order of the coherence length.

A natural question is how to detect the triplet components in this type of system. This can be achieved, for example, through spin-polarized spectroscopy [58]. Another way to detect the triplet components is to place a ferromagnetic layer (F) on top of a superconductor. The DOS of the F layer is modified by the superconducting correlations induced via the proximity effect. Such a modification can be measured by a normal tunneling probe. In the case of a weak proximity effect, we can linearize the Usadel equation in the F region. The DOS in the ferromagnet is then given by (see the Appendix for details)

$$\frac{N(\varepsilon, x, z)}{N_0} = 1 - \frac{1}{4}\mathrm{Re}\{\mathrm{Tr}\ \hat{f}^2(\varepsilon, x, z)\}. \tag{36}$$

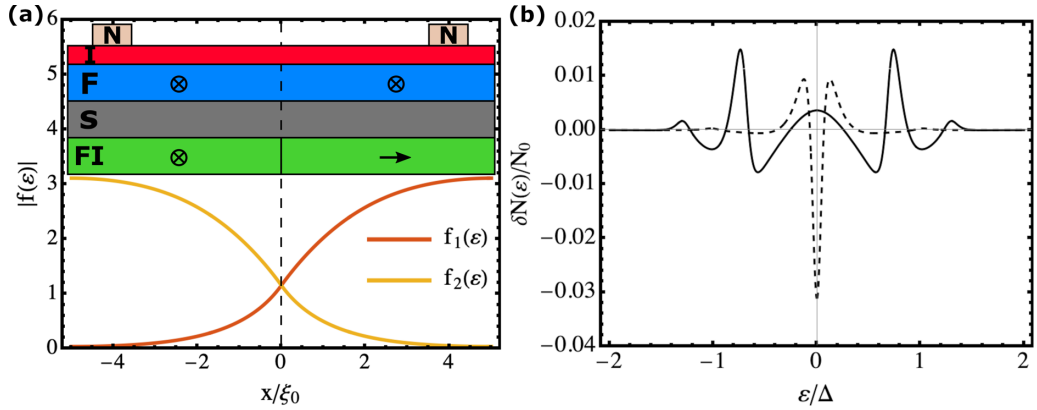

FIG. 6. (a) Spatial dependence of triplet correlations for energy $\varepsilon = \Delta - h$. We show the proposed geometry to detect the triplet correlations in the inset. An F layer is placed on top of an S layer; if the F layer is thick enough, only the triplet correlations perpendicular to the magnetization of the F layer will propagate along the ferromagnet. The long-range triplet correlations manifest as a zero-energy peak on the local DOS, measured through tunnel differential conductance measurements with a normal metal probe (N). (b) The correction to the DOS of the ferromagnet at the F/I interface, see panel (a), far to the right of the domain wall (solid line). The deviation from the normal DOS is due to the penetration of the long-range component of the triplet condensate. For comparison, we show the DOS of an N layer in contact with a conventional singlet superconductor (dashed line). At zero energy, the singlet (triplet) component induced in the N (F) layer is real (purely imaginary), resulting in a negative (positive) correction to the DOS. The parameters used in the plot are $h = 0.3\Delta$, $\gamma = 5\xi_0$, and $t = 3\xi_0$. The DOS of the F case is normalized by $(\Delta/\Gamma)^2$ for comparison.

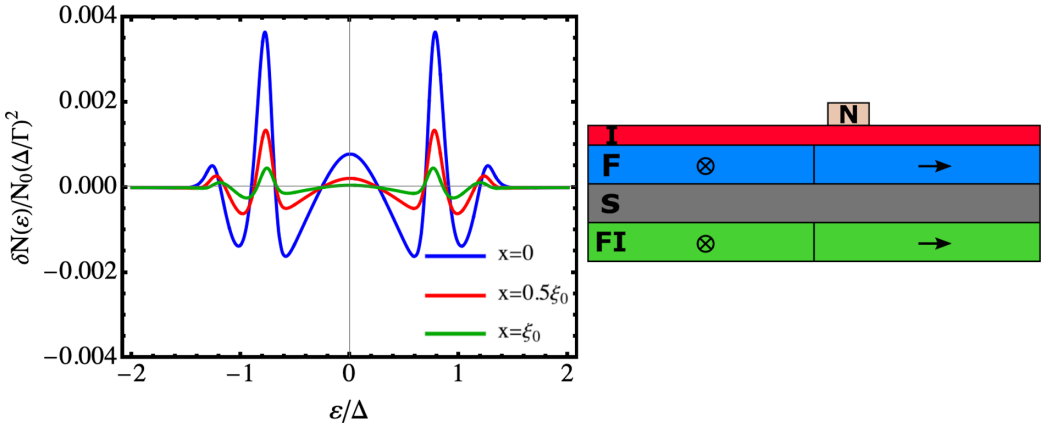

FIG. 7. Correction to the DOS of the ferromagnet at the F/I interface at different distances from the domain wall. In this setup, the ferromagnet magnetization is aligned with respect to the magnetization of the FI. The parameters used are $h = 0.3\Delta$, $\gamma = 5\xi_0$, and $t = 3\xi_0$.

The second term is the correction to the DOS due to the proximity effect. Because of the trace over spin, this term has two contributions: one proportional to the square of the singlet component, and one to the sum of the squares of the triplet components. The singlet component is real at low energies, so its correction to the DOS is negative. This explains that if S is a singlet superconductor and F is a normal layer (no exchange and hence no triplet), the DOS is suppressed at $\varepsilon = 0$; see the dashed line in Fig. 6(b). On the other hand, in the presence of an exchange field, the triplet component at $\varepsilon = 0$ is purely imaginary [see Eq. (A3)] and hence its contribution to the DOS, according to Eq. (36), is positive. Thus, the sign of the correction of the DOS at $\varepsilon = 0$ is determined by the competition between singlet and triplet amplitudes [59].

To separate the triplet from the singlet component, we propose a setup like the one sketched in Fig. 6. Due to the presence of the FI, triplet pairs are induced in the superconductor, as described above. To filter out the singlet correlations, an F layer with a magnetization noncollinear to the FI is placed; see the inset of Fig. 6(a). The singlet component and triplet parallel to the F magnetization (short-range triplet) decay over the magnetic length $\sim\kappa_F^{-1}$. In contrast, the triplet component orthogonal to the magnetization of F (long-range triplet) decays over the length $\sim\kappa_\varepsilon^{-1}$ (see Appendix). Thus, by choosing the thickness t of the F layer such that $\kappa_F^{-1} \ll t \ll \kappa_\varepsilon^{-1}$, the DOS of F at the tunneling barrier will only be corrected by the long-range triplet component. This situation can be realized by using F layers with a strong exchange field, such as Co or Fe.

In Appendix, we compute the correction to the density of states in the ferromagnet. In the two-domain situation studied above, when the F layer is placed above the right domain far from the domain wall [see Fig. 6(a)], the triplet component in F at zero energy is purely imaginary [Eq. (A3)], so according to Eq. (A4) there is a positive correction to the DOS,

$$\frac{N(0,\infty,t)}{N_0} = 1 + \frac{\varepsilon_b^2 h^2 \Delta^2}{2(\Delta^2 - h^2)^3}, \tag{37}$$

where $\varepsilon_b = D/(2\gamma t)$ is an energy scale related to the interface transparency, and γ is a parameter describing the interface resistance. The solid line in Fig. 6(b) shows the DOS of the F layer at the tunneling barrier computed for all energies. One sees a local maximum at $\varepsilon = 0$, and also maxima at $|\varepsilon| = \Delta \pm h$ related to the triplet peaks shown in Fig. 5. In this way, the existence of triplets generated in the spin-split superconductor can be demonstrated by performing tunneling spectroscopy, with the normal electrode probe; see Fig. 6(a).

Finally, we consider an F layer consisting of two domains that are collinear to the adjacent FI domains (see Fig. 7). This situation may correspond to the case in which the magnetic coupling of the F and FI leads to local collinear magnetizations. According to our previous analysis, triplet correlations of both kinds are present in the S near the domain wall. In other words, long-range triplet correlations will be present in certain positions of the F/I interface and affect the local DOS. In Fig. 7, we show the correction to the DOS at different points of the F/I interface. The zero-energy peak appears at regions close to the domain wall. The peak vanishes when moving away from the domain wall. Such measurements could be done with the help of the STM technique and may reveal the magnetic texture of the system. Another possible setup to isolate the odd-frequency correlations at zero energy are S/N bilayers with a spin-active interface [60,61].

VI. CONCLUSION

In this work, we have studied the spectral properties of superconductor-ferromagnetic insulator bilayers in the presence of a domain wall separating two magnetic domains. In the first part, we focus on the quasiparticle spectrum, and we analyze how the density of states of the superconductor is affected by the magnetic configuration. In the case of two semi-infinite domains with collinear magnetization and a sharp domain wall between them, it is possible to find two integrals of motion that allow for an analytical solution of the Usadel equation. With the help of this solution, we determine the local DOS of the superconductor for different magnitudes of the exchange field. At the domain wall, the DOS exhibits a "shark-fin" shape. This feature appears when the domain magnetizations are antiparallel or when one of the domains has a negligible small exchange field. We have also studied FI layers with noncollinear magnetization direction. We show that near the domain wall, the spin-splitting is quite robust with respect to the relative angle α between the magnetiza-

tions, but the heights of the coherent peaks are significantly affected by it. All these predictions can be verified by local tunnel spectroscopy experiments, which will reveal information about the local magnetic configuration of the FI.

In the second part, we have analyzed the spectral properties of the singlet and triplet components of the superconducting condensate in the S layer. We have found an analytical expression for the quasiclassical Green's function in the presence of an arbitrary magnetic texture in the FI in the case of a weak exchange field. Our expression reveals how the local exchange field spatially determines the triplet components induced in the superconductor. For arbitrary strength of the exchange interaction, we have determined the singlet and triplet components numerically in the presence of a sharp domain wall. We propose different ways of detecting the triplet correlations using a FI/S/F junction, where F is a ferromagnetic metal and a tunneling probe at the outer F interface. The presence of the triplet component manifests itself as a zero bias maximum in the tunneling differential conductance. The proposed setup can then be used as a source of spin-triplet pairs, whose entanglement can be proven in experiments using quantum dots as pair splitters [62].

ACKNOWLEDGMENTS

We thank S. Ilić for useful discussions. This work was partially funded by the Spanish Ministerio de Ciencia, Innovación y Universidades (MICINN) through Project No. PID2020-114252GB-I00 (SPIRIT), and EU's Horizon 2020 research and innovation program under Grant Agreement No. 800923 (SUPERTED). A.H. acknowledges funding by the University of the Basque Country (Project No. PIF20/05).

APPENDIX: CORRECTION TO THE TUNNELING DIFFERENTIAL CONDUCTANCE IN THE FERROMAGNET

In this Appendix, we show how the tunneling differential conductance measured on top of the F layer [see Fig. 6(a)] is affected by the leakage of the superconducting condensate into the ferromagnet.

The GF on a diffusive ferromagnet satisfies the Usadel equation (1) with $\Delta = 0$. If the transmission coefficient of the S/F interface is very low, the proximity effect in the F layer is weak and the Usadel equation can be linearized as

$$\partial_{zz}^2 f_0 + i\kappa_\varepsilon^2 f_0 - i\kappa_{\rm F}^2 f_2 = 0, \tag{A1a}$$

$$\partial_{zz}^2 \boldsymbol{f} + i\kappa_\varepsilon^2 \boldsymbol{f} - i\kappa_{\rm F}^2 f_0 \hat{\boldsymbol{y}} = 0, \tag{A1b}$$

where $\kappa_\varepsilon^2 = 2\varepsilon/D$, $\kappa_{\rm F}^2 = 2h_F/D$, and $h_{\rm F}$ is the field of the ferromagnet. Here we have assumed that the magnetization direction of the F layer lies on the y axis.

The S/F interface is described by the linearized Kuprianov-Lukichev condition [63],

$$\gamma\, \partial_z f_0|_{z=0} = -f_{{\rm S},0}, \tag{A2a}$$

$$\gamma\, \partial_z \boldsymbol{f}|_{z=0} = -\boldsymbol{f}_{\rm S}. \tag{A2b}$$

Here, $\gamma = \sigma_{\rm F} R_b$ is the parameter describing the barrier strength, where R_b is the normal-state tunneling resistance per unit area, and $\sigma_{\rm F}$ is the conductivity of the ferromagnet. The anomalous GF on the S layer is given by $\hat{f}_{\rm S} = f_{{\rm S},0} + \boldsymbol{f}_{\rm S} \cdot \boldsymbol{\sigma}$.

We assume that the thickness t of the F layer is much longer than the coherence length in the ferromagnetic layer $\kappa_{\rm F} t \gg 1$. In the long-junction regime, the condensate function is mediated primarily by the long-range triplet superconducting correlations [35,64,65], whereas the singlet and short-range triplet correlations decay over the length $\kappa_{\rm F}^{-1}$. At the outer interface of the F layer, the condensate function is given by the only long-range component f_1. Solving the Usadel equation (A1b), we obtain

$$f_1(\varepsilon, x, t) = \frac{f_{{\rm S},1}(\varepsilon, x)}{\frac{1-i}{\sqrt{2}}\kappa_\varepsilon \gamma \sinh\left(\frac{1-i}{\sqrt{2}}\kappa_\varepsilon t\right)}. \tag{A3}$$

In the case of the weak proximity effect, the DOS of the ferromagnet is given by Eq. (36). Using Eq. (A3), we arrive at

$$\frac{N(\varepsilon, x, t)}{N_0} = 1 - \frac{1}{2}{\rm Re}\left\{\frac{i f_{{\rm S},1}(\varepsilon, x)^2}{\gamma^2 \kappa_\varepsilon^2 \sinh^2\left(\frac{1-i}{\sqrt{2}}\kappa_\varepsilon t\right)}\right\}, \tag{A4}$$

where the anomalous GF of the superconductor $f_{{\rm S},1}(\varepsilon, x)$ is obtained by solving Eqs. (30) and (31). If the S layer is a homogeneous superconductor with an exchange field along the x direction, the DOS is given by Eq. (37).

[1] J. S. Moodera, X. Hao, G. A. Gibson, and R. Meservey, Phys. Rev. Lett. **61**, 637 (1988).
[2] X. Hao, J. S. Moodera, and R. Meservey, Phys. Rev. B **42**, 8235 (1990).
[3] R. Meservey and P. Tedrow, Phys. Rep. **238**, 173 (1994).
[4] E. Strambini, V. N. Golovach, G. De Simoni, J. S. Moodera, F. S. Bergeret, and F. Giazotto, Phys. Rev. Materials **1**, 054402 (2017).
[5] A. Hijano, S. Ilić, M. Rouco, C. González-Orellana, M. Ilyn, C. Rogero, P. Virtanen, T. T. Heikkilä, S. Khorshidian, M. Spies, N. Ligato, F. Giazotto, E. Strambini, and F. S. Bergeret, Phys. Rev. Research **3**, 023131 (2021).
[6] G.-X. Miao, J. Chang, B. A. Assaf, D. Heiman, and J. S. Moodera, Nat. Commun. **5**, 3682 (2014).
[7] G. De Simoni, E. Strambini, J. S. Moodera, F. S. Bergeret, and F. Giazotto, Nano Lett. **18**, 6369 (2018).
[8] K.-R. Jeon, J.-C. Jeon, X. Zhou, A. Migliorini, J. Yoon, and S. S. P. Parkin, ACS Nano **14**, 15874 (2020).
[9] R. Ojajärvi, T. T. Heikkilä, P. Virtanen, and M. A. Silaev, Phys. Rev. B **103**, 224524 (2021).
[10] M. Alidoust, K. Halterman, and J. Linder, Phys. Rev. B **88**, 075435 (2013).
[11] E. Strambini, F. Bergeret, and F. Giazotto, Europhys. Lett. **112**, 17013 (2015).
[12] F. Giazotto, T. T. Heikkilä, A. Luukanen, A. M. Savin, and J. P. Pekola, Rev. Mod. Phys. **78**, 217 (2006).
[13] F. Giazotto, P. Solinas, A. Braggio, and F. S. Bergeret, Phys. Rev. Applied **4**, 044016 (2015).

[14] F. Giazotto and F. Bergeret, Appl. Phys. Lett. **102**, 132603 (2013).

[15] F. Giazotto, T. T. Heikkilä, and F. S. Bergeret, Phys. Rev. Lett. **114**, 067001 (2015).

[16] F. Giazotto and F. Bergeret, Appl. Phys. Lett. **116**, 192601 (2020).

[17] P. Machon, M. Eschrig, and W. Belzig, Phys. Rev. Lett. **110**, 047002 (2013).

[18] A. Ozaeta, P. Virtanen, F. S. Bergeret, and T. T. Heikkilä, Phys. Rev. Lett. **112**, 057001 (2014).

[19] T. T. Heikkilä, R. Ojajärvi, I. J. Maasilta, E. Strambini, F. Giazotto, and F. S. Bergeret, Phys. Rev. Applied **10**, 034053 (2018).

[20] Z. Geng, A. P. Helenius, T. T. Heikkilä, and I. J. Maasilta, J. Low Temp. Phys. **199**, 585 (2020).

[21] Y. Oreg, G. Refael, and F. von Oppen, Phys. Rev. Lett. **105**, 177002 (2010).

[22] R. M. Lutchyn, J. D. Sau, and S. Das Sarma, Phys. Rev. Lett. **105**, 077001 (2010).

[23] X.-F. Dai, X.-Q. Wang, T. Gong, L.-L. Zhang, and W. Gong, J. Phys. E **128**, 114585 (2021).

[24] J. S. Moodera, T. S. Santos, and T. Nagahama, J. Phys.: Condens. Matter **19**, 165202 (2007).

[25] T. Tokuyasu, J. A. Sauls, and D. Rainer, Phys. Rev. B **38**, 8823 (1988).

[26] P. Virtanen, A. Vargunin, and M. Silaev, Phys. Rev. B **101**, 094507 (2020).

[27] M. Rouco, S. Chakraborty, F. Aikebaier, V. N. Golovach, E. Strambini, J. S. Moodera, F. Giazotto, T. T. Heikkilä, and F. S. Bergeret, Phys. Rev. B **100**, 184501 (2019).

[28] A. Y. Aladyshkin, A. I. Buzdin, A. A. Fraerman, A. S. Mel'nikov, D. A. Ryzhov, and A. V. Sokolov, Phys. Rev. B **68**, 184508 (2003).

[29] M. Houzet and A. I. Buzdin, Phys. Rev. B **74**, 214507 (2006).

[30] I. V. Bobkova and A. M. Bobkov, JETP Lett. **109**, 57 (2019).

[31] D. S. Rabinovich, I. V. Bobkova, A. M. Bobkov, and M. A. Silaev, Phys. Rev. B **99**, 214501 (2019).

[32] F. Aikebaier, P. Virtanen, and T. Heikkilä, Phys. Rev. B **99**, 104504 (2019).

[33] Z. Yang, M. Lange, A. Volodin, R. Szymczak, and V. V. Moshchalkov, Nat. Mater. **3**, 793 (2004).

[34] J. Linder and K. Halterman, Phys. Rev. B **90**, 104502 (2014).

[35] F. S. Bergeret, A. F. Volkov, and K. B. Efetov, Rev. Mod. Phys. **77**, 1321 (2005).

[36] A. Cottet, Phys. Rev. Lett. **107**, 177001 (2011).

[37] F. S. Bergeret, M. Silaev, P. Virtanen, and T. T. Heikkilä, Rev. Mod. Phys. **90**, 041001 (2018).

[38] T. T. Heikkilä, M. Silaev, P. Virtanen, and F. S. Bergeret, Prog. Surf. Sci. **94**, 100540 (2019).

[39] K. D. Usadel, Phys. Rev. Lett. **25**, 507 (1970).

[40] F. S. Bergeret, A. Verso, and A. F. Volkov, Phys. Rev. B **86**, 214516 (2012).

[41] M. Eschrig, A. Cottet, W. Belzig, and J. Linder, New J. Phys. **17**, 083037 (2015).

[42] X.-P. Zhang, F. S. Bergeret, and V. N. Golovach, Nano Lett. **19**, 6330 (2019).

[43] B. S. Chandrasekhar, Appl. Phys. Lett. **1**, 7 (1962).

[44] A. M. Clogston, Phys. Rev. Lett. **9**, 266 (1962).

[45] D. A. Ivanov and Y. V. Fominov, Phys. Rev. B **73**, 214524 (2006).

[46] A. Kamenev, *Field Theory of Non-Equilibrium Systems* (Cambridge University Press, Cambridge, 2011), Chap. 14.

[47] A. Altland and B. Simons, *Condensed Matter Field Theory*, 2nd ed. (Cambridge University Press, Cambridge, 2010), Chap. 1.

[48] A. Altland, B. D. Simons, and D. T. Semchuk, Adv. Phys. **49**, 321 (2000).

[49] A. A. Golubov, M. Y. Kupriyanov, and M. Siegel, J. Exp. Theor. Phys. **81**, 180 (2005).

[50] Domain walls with noncollinear magnetization may induce stray fields that could affect superconductivity. In this work, we neglect the orbital effects of stray fields and assume that the superconducting gap is homogeneous in the S layer. The stray fields depend on the geometry and size of the magnetic layer, so we assume that the FI geometry is such that it minimizes the magnetostatic energy and, therefore, the stray fields. For any angle α, the stray field can be minimized if the orientation of the domains is chosen to be $\pm\alpha/2$ with respect to the x axis.

[51] T. E. Baker, A. Richie-Halford, and A. Bill, Phys. Rev. B **94**, 104518 (2016).

[52] F. S. Bergeret, A. F. Volkov, and K. B. Efetov, Phys. Rev. Lett. **86**, 4096 (2001).

[53] V. L. Berezinskii, Sov. J. Exp. Theor. Phys. Lett. **20**, 628 (1974).

[54] Y. Tanaka, M. Sato, and N. Nagaosa, J. Phys. Soc. Jpn. **81**, 011013 (2012).

[55] J. Linder and A. V. Balatsky, Rev. Mod. Phys. **91**, 045005 (2019).

[56] M. Eschrig, Phys. Today **64**(1), 43 (2011).

[57] R. C. Dynes, V. Narayanamurti, and J. P. Garno, Phys. Rev. Lett. **41**, 1509 (1978).

[58] I. V. Bobkova, A. M. Bobkov, and W. Belzig, New J. Phys. **21**, 043001 (2019).

[59] T. Yokoyama, Y. Tanaka, and A. A. Golubov, Phys. Rev. B **75**, 134510 (2007).

[60] J. Linder, T. Yokoyama, A. Sudbø, and M. Eschrig, Phys. Rev. Lett. **102**, 107008 (2009).

[61] J. Linder, A. Sudbø, T. Yokoyama, R. Grein, and M. Eschrig, Phys. Rev. B **81**, 214504 (2010).

[62] L. Hofstetter, S. Csonka, J. Nygård, and C. Schönenberger, Nature (London) **461**, 960 (2009).

[63] M. Y. Kuprianov and V. F. Lukichev, Zh. Eksp. Teor. Fiz. **94**, 139 (1988) [Sov. Phys. JETP **67**, 1163 (1988)].

[64] A. I. Buzdin, A. S. Mel'nikov, and N. G. Pugach, Phys. Rev. B **83**, 144515 (2011).

[65] A. V. Samokhvalov, J. W. A. Robinson, and A. I. Buzdin, Phys. Rev. B **100**, 014509 (2019).